

A Flexible, Reaction-Wheel-Driven Fish Robot: Flow Sensing and Flow-Relative Control

Feitian Zhang, Patrick Washington and Derek A. Paley

Abstract—This paper studies flow sensing and flow-relative control for a flexible fish robot actuated by an internal reaction wheel. Two flow models are presented including a quasi-steady potential flow model and an unsteady vortex-shedding model. A recursive Bayesian filter is adopted to assimilate distributed pressure measurements and a bending-curvature measurement for flow-field estimation. The dynamic model of the reaction-wheel-driven fish robot is derived. A flow-relative control strategy for tracking swimming speed and turning rate consists of a feedforward controller designed based on the inverse steady-state turning model and a feedback controller that utilizes estimated flow information and an angular velocity measurement. Simulation results are presented to demonstrate the control design.

I. INTRODUCTION

Fish attract scientific attention for their superior swimming maneuverability and energy-efficiency. Over the past two decades, scientists and engineers have made great efforts in designing and developing bio-inspired fish robots to improve the performance of existing underwater vehicles [1], [2].

Many fish-robot designs follow a two-segment (or multi-segment) profile. The frontal segment(s), usually made rigid, hold electronics components, and the posterior segment, flaps for propulsion. Although the two-segment robot design generates fish-like swimming motion, the partitioned body fundamentally performs articulated robot dynamics involving hydrodynamic interactions with water, which may limit agility and increase energy cost.

Recently, actuation using an internal rotor for a rigid swimming robot has been reported [3]. The rotor is mounted inside the fish robot and includes a large, spinning disk. Following a periodic angular-velocity profile, the internal rotor generates torque that flaps the fish robot. Propulsion using an internal rotor allows the fish robot to be designed and actuated as a whole body. It also reduces the risk of external actuator failure due to servo deterioration when operated in fluid. However, the design in [3] adopts a large inertia for the rotor, which requires large space inside the robot. Correspondingly, the spinning speed of the internal rotor is slow, which leads to strong dynamic coupling between the rotor and the robot, and thus a complicated moment-control problem (not described in [3]).

This work was supported by ONR Grant No. N000141410249.

F. Zhang, P. Washington and D. Paley are with the Department of Aerospace Engineering and Institute for Systems Research, University of Maryland, College Park, MD, 20742, USA. Email: feitian.zhang@outlook.com (Zhang), phw@umd.edu (Washington), dpaley@umd.edu (Paley).

Send correspondence to D. Paley. Tel: (301) 405-575, Fax: (301) 314-0213.

This paper proposes a novel fish-robot actuation approach using an internal fast-spinning reaction wheel for a flexible Joukowski-shaped fish robot. A reaction wheel is a type of flywheel used primarily by spacecraft for attitude control [4]. When its rotation speed is changed, the spacecraft will counter-rotate proportionately through conservation of angular momentum. A reaction wheel can only rotate a spacecraft; it is not capable of moving the spacecraft from one place to another. When using a reaction wheel in a fish robot, the relative rotation between the robot and the surrounding fluid generates hydrodynamic forces and moments that propel the fish robot. A flexible body deforms by bending, which may help with propulsion. We set the angular speed of the reaction wheel much greater than the angular speed of the fish robot so that the motion control of the reaction wheel is nearly decoupled from the robot. The effect of the reaction wheel can then be interpreted as an external control moment acting on the fish robot, which simplifies the robot control design and potentially benefits higher-level tasks, such as path planning and multi-agent cooperation.

Fish have a sensory organ called the lateral line to detect surrounding flow and are capable of navigating in unknown, murky, and cluttered environments [5]. Many underwater vehicles detect global flow speed rather than local velocity using an acoustic Doppler current profiler, which is too large and expensive for small robots. Some researchers have been studying the fabrication and usage of an artificial lateral line for flow sensing of underwater robots [6]–[8]. Our previous work [7] has demonstrated successful flow sensing using distributed pressure sensors in constrained one-dimensional speed control of a servo-actuated fish robot. This paper extends the previous study to include flow-relative-speed and turning-rate control in two-dimensional free swimming with a flexible fish robot actuated by a reaction wheel. In addition to distributed pressure measurements along the robot body, we include a measurement of the body curvature (sensed by commercially available flex-sensors) to enhance state estimation, and an angular-velocity measurement of the robot body orientation (sensed by a single-axis gyroscope) for flow-relative control.

This paper briefly reviews two flow models for a cambered-Joukowski foil: a quasi-steady potential flow model and an unsteady vortex-shedding model. Based on its tractability and accuracy, the quasi-steady potential flow model is used in a recursive Bayesian filter that assimilates distributed pressure and curvature measurements to estimate the flow, whereas the unsteady vortex-shedding model is used for simulating the ground-truth flow field. We derive

a dynamic model of the fish robot driven by an internal reaction-wheel whose control torque profile follows a biased sinusoidal waveform. The deformation of the flexible body is modeled using a time-varying parameter (the camber ratio). For flow-relative path-following, we propose a control strategy to track flow-relative swimming speed and flow-relative turning rate, which combines a feedforward controller designed based on the inverse steady-state turning model and a feedback controller that utilizes estimated flow and measured angular velocity. Simulations are conducted in a uniform flow to demonstrate the control strategy.

II. FLOW MODEL FOR A CAMBERED JOUKOWSKI-SHAPED FISH ROBOT

This paper adopts the shape of a Joukowski foil for the design of the fish robot in order to utilize potential-flow theory. In fluid dynamics, potential-flow theory [9] describes the velocity field as the gradient of a scalar function, the velocity potential, which is applicable to incompressible, irrotational flow. This section briefly reviews two models of flow past a cambered Joukowski foil: the quasi-steady potential-flow method and the unsteady vortex-shedding method [7].

A. Quasi-steady Potential-Flow Model

The fish robot modeled as a Joukowski foil takes the shape of the output of the Joukowski transformation of a circle. The Joukowski transformation, a conformal mapping, is expressed as [7], [9]

$$z = \xi + \frac{a^2}{\xi} + z_C, \quad (1)$$

where the set of points ξ represents a circle with radius R centered at ξ_0 in the complex ξ -plane. The Joukowski transformation parameter a is approximately one quarter of the chord length of the foil l . The image of the mapping in the z -plane defines the boundary of the fish robot $z = x + iy$ (Fig. 1). The origin O of the z -plane is the center of rotation for the flapping motion, chosen to be the one-quarter point along the camber line, as measured from the leading edge. The x -axis runs parallel to the chord line from the leading edge to the trailing edge. z_C is the z -plane coordinate of the center point of the chord line C . We define the z -plane as the body-fixed frame.

A two-dimensional fluid with relative velocity U flows past the foil-shaped fish robot. The angle between the x -axis and the direction of the relative velocity U is the angle-of-attack α , with the nose pitching up chosen to be the positive direction (Fig. 1).

According to potential-flow theory, the flow in the complex circle plane (ξ -plane) prescribes the flow in the corresponding foil plane (z -plane) via a conformal map. In an inviscid, incompressible, and irrotational fluid, the quasi-steady complex potential of the flow in the ξ -plane is a function of the relative flow speed U , the angle-of-attack α , the radius R , and the center ξ_0 . The complex potential [9]

$$W(\xi) = U(\xi - \xi_0)e^{-i\alpha} + U\frac{R^2}{\xi - \xi_0}e^{i\alpha} + i\frac{\Gamma}{2\pi}\ln(\xi - \xi_0), \quad (2)$$

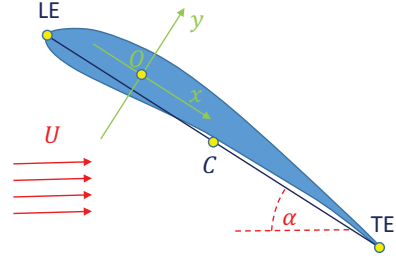


Fig. 1: Illustration of Joukowski-shaped fish robot and the body-fixed reference frames O . TE is the trailing edge and LE is the leading edge.

represents the sum of three elementary flow fields: a uniform flow, a doublet, and a point vortex located at the center of the circle. The vortex circulation Γ is evaluated by enforcing the Kutta condition [9], which requires the trailing edge to be a stagnation point. The vortex circulation is [9]

$$\Gamma = 4\pi RU \sin(\alpha + \beta). \quad (3)$$

Here $\beta = \arcsin(x_{\xi_0}/R)$ is the phase angle of the center point ξ_0 . Under the assumption that $|\xi_0| \ll a$, β is approximated by $2H$. Here $H = y_{\xi_0}/(2a)$ is the camber ratio of the Joukowski foil, which intuitively describes how much the foil bends.

With the quasi-steady potential-flow model, we calculate the flow field around the fish robot, given any parameter set (U, α, H) [7].

B. Vortex-shedding Flow Model

The quasi-steady potential-flow model does not describe the unsteady or transient effects caused by the flapping motion of a flexible fish robot. This subsection presents a second flow model, used for simulating the flow field, that features discrete-time vortex shedding [10]. In this model, a new vortex is shed into the flow from the trailing edge of the foil at every discrete time step.

Let Ω be the angular velocity of the fish robot with counter-clockwise rotation about the pivot point O chosen to be the positive direction ($\dot{\alpha} = -\Omega$). In the vortex-shedding model, the complex flow potential with respect to the ξ -plane is [7]

$$W = U(\xi - \xi_0)e^{-i\alpha} + U\frac{R^2}{\xi - \xi_0}e^{i\alpha} + \Omega W_\Omega + i\frac{\Gamma_0}{2\pi}\ln\frac{\xi - \xi_0}{R} + \sum_{k=1}^n i\frac{\Gamma_k}{2\pi}\left(\ln(\xi - \xi_k) - \ln\left(\xi - \xi_0 - \frac{R^2}{\xi_k - \xi_0}\right)\right). \quad (4)$$

The corresponding unit complex potential is denoted by W_Ω . Γ_0 represents the vortex circulation at the center of the circle and Γ_k represents the circulation of the k^{th} vortex located at position ξ_k .

To speed up simulation, we discard all vortices shed prior to last three flapping time periods. The effects of deleted vortices on the fish robot are reflected in the new shed vortex by applying the Kutta condition [9].

III. DYNAMIC MODEL OF A FLEXIBLE FISH ROBOT WITH REACTION-WHEEL ACTUATION

This section studies the dynamics of a flexible fish robot actuated by an internal reaction wheel that spins at high RPM in the same direction of the rotational motion of the fish robot through the origin O . First, we define the inertial reference frame A such that the x^I -axis is along the opposite direction of the initial velocity of the fish robot at $t = 0$. Define θ as the rotation angle from the inertial frame to the body-fixed frame. Let $\mathbf{\Pi} = \mathbf{J}\omega + \mathbf{J}_r(\omega + \omega_r)$ and $\mathbf{P} = \mathbf{M}\mathbf{v}$ denote the total angular and linear momenta of the robot-fluid-reaction-wheel system, respectively, where ω is the angular velocity of the body-fixed frame with respect to the inertial frame expressed in the body-fixed frame, \mathbf{v} is the corresponding translational velocity with an amplitude of V , ω_r is the angular velocity of the reaction wheel with respect to the body-fixed frame, \mathbf{J}_r is the inertia matrix of the reaction wheel, \mathbf{J} is the inertia matrix of the fish robot, and \mathbf{M} is the mass matrix. Both \mathbf{J} and \mathbf{M} include the added mass, which describes the additional effect (force) resulting from water acting on the fish robot during acceleration or deceleration. Assume the off-diagonal terms in the inertia matrix are negligible and the added mass and added inertia do not vary significantly during the flapping motion. The dynamics of the fish robot are governed by Kirchhoff's equations [11], i.e.,

$$\dot{\mathbf{\Pi}} = \mathbf{\Pi} \times \omega + \mathbf{P} \times \mathbf{v} + \mathbf{T} \quad (5)$$

$$\dot{\mathbf{P}} = \mathbf{P} \times \omega + \mathbf{F}, \quad (6)$$

where \mathbf{T} is the external moment vector and \mathbf{F} is the external force vector.

For the planar motion of the fish robot, which is the focus of this paper, we have

$$\begin{aligned} \omega &= [0, 0, \Omega]^T, & \omega_r &= [0, 0, \Omega_r]^T, & \mathbf{M} &= \text{diag}(m_1, m_2, m_3), \\ \mathbf{v} &= [v_1, v_2, 0]^T, & \mathbf{T} &= [0, 0, T_p]^T, & \mathbf{P} &= [m_1 v_1, m_2 v_2, 0]^T, \\ \mathbf{F} &= [-(F_t - F_d \cos \alpha + F_l \sin \alpha), F_l \cos \alpha + F_d \sin \alpha, 0]^T, \\ \text{and } \mathbf{\Pi} &= [0, 0, J\Omega + J_r(\Omega + \Omega_r)]^T. \end{aligned}$$

Here J is the sum of the inertia of the robot and the added inertia in the pitching direction, J_r is the pitching component of the locked inertia of the reaction wheel, and m_1 and m_2 are the sum of the mass of the robot and the added mass in the directions of surge and sway, respectively.

Figure 2 illustrates the hydrodynamic pitching torque T_p , the thrust force F_t , generated by the flapping motion of the foil with the $-x$ -axis direction as positive, the drag force F_d , in the opposite direction of the motion of the robot relative to the fluid, and the lift force F_l , perpendicular to the relative-flow direction. The flow speed with respect to the inertial frame is denoted by \mathbf{U}_f . The relative velocity of the flow with respect to the robot is $\mathbf{U} = \mathbf{U}_f + \mathbf{v}$ with an amplitude U .

Define the control torque of the reaction wheel as T_r , so the calculation reads

$$T_r = \frac{d}{dt}(J_r(\Omega + \Omega_r)). \quad (7)$$

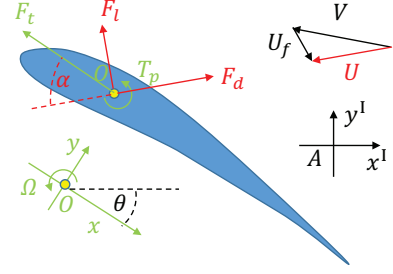


Fig. 2: Schematic of hydrodynamic forces and moments.

Assuming the change rate of the angular velocity of the reaction wheel is much greater than that of the fish robot, the control torque is approximately

$$T_r = \frac{d}{dt}(J_r \Omega_r). \quad (8)$$

The dynamics (5) and (6) for planar motion in first-order form are

$$J\dot{\Omega} = (m_1 - m_2)v_1 v_2 + T_p - T_r \quad (9)$$

$$m_1 \dot{v}_1 = m_2 v_2 \Omega - (F_t - F_d \cos \alpha + F_l \sin \alpha) \quad (10)$$

$$m_2 \dot{v}_2 = -m_1 v_1 \Omega + F_l \cos \alpha + F_d \sin \alpha. \quad (11)$$

The kinematics equations are

$$\dot{\theta} = \Omega \quad (12)$$

$$\dot{x} = v_1 \cos \theta - v_2 \sin \theta \quad (13)$$

$$\dot{y} = v_1 \sin \theta + v_2 \cos \theta, \quad (14)$$

where x and y are the coordinates of the body-fixed-frame origin O in the inertial frame.

The hydrodynamic forces and moment are modeled following aerospace engineering conventions [12], i.e.,

$$T_p = C_p(\alpha + 2H)U^2 - K_p \Omega \quad (15)$$

$$F_d = (C_d^0 + C_d(\alpha + 2H)^2)U^2 \quad (16)$$

$$F_l = C_l(\alpha + 2H)U^2, \quad (17)$$

where C_p , C_d^0 , C_d , and C_l are hydrodynamic coefficients that can be identified using flow tunnel experiments, and K_p is the pitch-damping coefficient.

Select the sum of a sinusoidal waveform and a linear function for the control profile of the reaction-wheel spinning speed to achieve the periodic flapping motion, i.e.,

$$\Omega_r = A \sin \phi + Bt = A \sin(2\pi ft) + Bt, \quad (18)$$

where ϕ is the phase angle of the periodic sinusoidal component of the angular velocity Ω_r of the reaction wheel, f is the oscillating frequency, A is the oscillating amplitude, and B is the bias rate. The control torque is then

$$T_r = 2\pi f A \sin \phi + B = 2\pi f A \sin(2\pi ft) + B. \quad (19)$$

From the conservation law of angular momentum, the fish robot will flap following the same driving frequency with an amplitude proportional to the oscillation amplitude A .

The thrust force generated by the periodic actuation (19) is approximated as [2]

$$F_t = \bar{F}_t + (\hat{F}_t - \bar{F}_t) \sin(2\phi), \quad (20)$$

where \bar{F}_t and \hat{F}_t are the mean and maximum thrust force in one flapping period, respectively. The mean and maximum thrust force depend on the product of the amplitude and frequency of the flapping motion [2], i.e.,

$$\bar{F}_t = k_1 (Af)^{k_2} \quad (21)$$

$$\hat{F}_t = k_3 (Af)^{k_4}. \quad (22)$$

The parameters k_1 , k_2 , k_3 , and k_4 are identified by force-sensing experiments (k_2 and k_4 are approximately equal to 2 [2]).

Modeling camber dynamics is a challenging fluid-structure-interaction problem that may involve continuum mechanics and boundary-value partial differential equations. However, we use a tractable model to capture the camber motion for the purpose of real-time control. Suppose the camber kinematics are a linear function of the second derivative of the pitch angle with respect to time, i.e.,

$$\dot{H} = -K_h \ddot{\theta} = -K_h \dot{\Omega}, \quad (23)$$

where K_h is the camber-dynamics coefficient.

IV. FLOW SENSING USING DISTRIBUTED PRESSURE AND BENDING SENSORS

Flow estimation for underwater robots is a challenging problem, especially for low-speed operations. This section describes a distributed flow-sensing algorithm using a Bayesian filter. The algorithm assimilates distributed pressure measurements and a bending curvature measurement to estimate the relative flow speed U , the angle-of-attack α , and the camber ratio H for the purpose of closed-loop control.

Consider a flexible fish robot equipped with N_p pressure sensors located at positions z_{p_i} , $i = 1, \dots, N_p$, and a bending sensor along the camber line of the Joukowski-shaped fish. The bending sensor measures the average bending curvature κ of the body, which is linearly dependent on the camber ratio H ,

$$\kappa = C_\kappa H; \quad (24)$$

the coefficient C_κ is identified in sensor calibration. Each pressure sensor measures the local static pressure modeled by Bernoulli's equation for inviscid, incompressible flow along a streamline [9]:

$$p_i = C - \rho \frac{\partial \phi(z_{p_i})}{\partial t} - \frac{1}{2} \rho |f(z_{p_i})|^2, \quad (25)$$

where p_i is the predicted static pressure at location z_{p_i} , $f(z_{p_i})$ is the local flow velocity, ρ is the water density, and C is a constant; $\phi = (W + \bar{W})/2$ is the time-dependent velocity potential.

Similar to the lateral-line system in fish [5], the pressure differences between each sensor pair form the individual flow measurement of the fish robot. We assume a quasi-steady

flow for estimation purposes, meaning there is no unsteady effect. The flow measurement equation is [8], [13]

$$\Delta p_{ij} = p_i - p_j = \frac{1}{2} \rho (|f(z_{p_j})|^2 - |f(z_{p_i})|^2). \quad (26)$$

There are $N_m = (N_p)!/2!/(N_p - 2)!$ possible measurements in total, i.e., the combinatorial number of sensor pairs. Define $\mathbf{z}_p = [z_1, \dots, z_{N_p}]^T$, $\Delta \mathbf{p} = [\Delta p_{12}, \dots, \Delta p_{1N_p}, \Delta p_{23}, \dots, \Delta p_{2N_p}, \dots, \Delta p_{N_p-1N_p}]^T$ and $\mathbf{m}_s = [\Delta \mathbf{p}, \kappa]^T$ to be the vectors representing sensor locations, pressure difference pairs, and total sensor measurements respectively. Assuming the sensor measurements of the fish robot \mathbf{m}_s are corrupted with Gaussian noise, then the actual i th element of the measurement vector is

$$\tilde{\mathbf{m}}_s(i) = \mathbf{m}_s(i) + \eta_i, \quad (27)$$

where $\eta_i \sim N(0, \sigma_i^2)$ is drawn from a zero-mean Gaussian distribution with variance σ_i .

Given the sensor measurements, a flow model for the flapping fish robot is used to reconstruct the flow field. Although the vortex-shedding model is a reliable model for describing the flow field, the discrete-time vortex addition is not suitable for real-time feedback control. A more tractable model is the quasi-steady potential-flow model. Let $\mathbf{\Lambda} = [U, \alpha, H]^T$ represent the flow parameter vector. The Bayesian estimate of $\mathbf{\Lambda}$ is based on distributed flow measurements and bending curvature measurement.

The Bayesian filter, also known as a recursive Bayesian estimator [14], is a general probabilistic approach for estimating an unknown probability density function (pdf) recursively over time using incoming measurements and a mathematical process model. The sensor measurements $\tilde{\mathbf{m}}_s$ are assimilated recursively at each step to infer the most likely parameter vector $\hat{\mathbf{\Lambda}}$. The Bayesian formula for calculating the posterior probability of the flow parameters from the acquired measurements is [14]

$$p(\mathbf{\Lambda}(t)|\mathbf{D}(t)) = \gamma p(\tilde{\mathbf{m}}_s|\mathbf{\Lambda}) p(\mathbf{\Lambda}(t)|\mathbf{D}(t - \Delta t)), \quad (28)$$

where $p(\tilde{\mathbf{m}}_s|\mathbf{\Lambda})$ is the likelihood function of the new measurements $\tilde{\mathbf{m}}_s$ given the parameters $\mathbf{\Lambda}$, $p(\mathbf{\Lambda}(t)|\mathbf{D}(t))$ and $p(\mathbf{\Lambda}(t)|\mathbf{D}(t - \Delta t))$ are the posterior and prior pdf for time t , respectively, $\mathbf{D}(t) = \{\tilde{\mathbf{m}}_s(t), \tilde{\mathbf{m}}_s(t - \Delta t), \dots, \tilde{\mathbf{m}}_s(0)\}$ represents all sensor measurements up to time t , and γ is the coefficient that ensures the total probability of the posterior over the parameter space is equal to 1. This paper uses a grid-based Bayesian filter rather than a particle filter to discretize the parameter space.

The assumption of Gaussian noise in the flow measurements leads to a Gaussian likelihood function,

$$p(\tilde{\mathbf{m}}_s(i)|\mathbf{\Lambda}) = \frac{1}{\sqrt{2\pi}\sigma_i} \exp\left(-\frac{1}{2\sigma_i^2}(\mathbf{m}_s(i) - \tilde{\mathbf{m}}_s(i))^2\right), \quad (29)$$

where $i = 1, \dots, N_m + 1$ is the index for the i th element of the sensor measurement vector $\tilde{\mathbf{m}}_s$.

V. FLOW-RELATIVE CONTROL USING INTERNAL REACTION WHEEL

This section presents the closed-loop controller design for flow-relative path-following. The objective is to control the flow-relative speed U and flow-relative turning rate ω^U of a flexible fish robot by tuning the amplitude A and bias rate B of the periodic oscillation of a fast-spinning, internal reaction wheel. Flow-relative control is important for the navigation of fish robots in unknown and cluttered environments; it also facilitates higher-level control tasks such as path planning and multi-agent cooperation.

We propose a feedforward-feedback control scheme (Fig. 3) for the path-following problem. The feedforward term aims to speed up tracking by providing open-loop control based on the inverse steady-state turning model. The feedback term aims to guarantee stability and reduce tracking error based on the flow Bayesian estimate and angular velocity measurement.

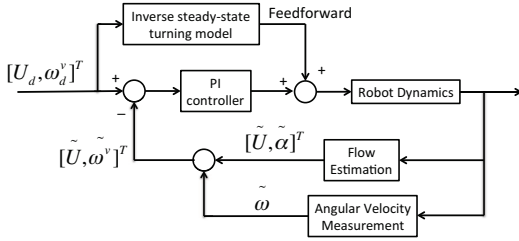


Fig. 3: Block diagram for the closed-loop control system, combining feedforward and feedback control.

For steady-state turning motion of a fish robot, the control variables (the amplitude A and bias rate B) in the reaction-wheel angular-velocity equation (18) satisfy the balance equations of force and moment [15]

$$\bar{F}_t = F_d \quad (30)$$

$$T_p = T_r, \quad (31)$$

where the mean thrust force \bar{F}_t is equal to the drag force F_d and the control torque T_r of the reaction wheel is equal to the hydrodynamic pitching moment T_p . We further assume the mean angle-of-attack over a flapping period is zero because the angle-of-attack, usually less than 0.25, has minor influence on the drag force and pitch moment in steady turning. Although this steady-state turning model ignores transient dynamics during the flapping period, the prediction for turning motion based on this simplified model is relatively accurate [15]. Given desired flow-relative speed U_d and turning rate ω_d^U , the feedforward controls are analytical and easy to implement, i.e.,

$$A_f = \frac{1}{f} \left(\frac{C_d^0 U_d^2}{k_1} \right)^{\frac{1}{k_2}}, \quad (32)$$

$$B_f = \frac{K_p \omega_d^U}{J_r}, \quad (33)$$

where A_f and B_f are the feedforward components of control variables A and B , respectively.

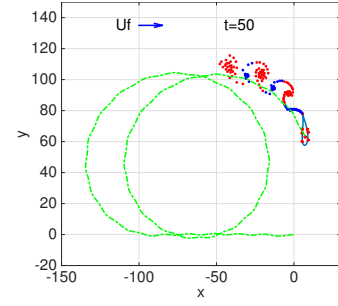


Fig. 4: Flow-relative control trajectory of the fish robot using the vortex-shedding method in a uniform flow with a speed of 1 cm/s.

Feedback control utilizes estimated flow information (\tilde{U} and $\tilde{\alpha}$) obtained from the recursive Bayesian filter and the estimated angular velocity $\tilde{\omega}$ measured from a single-axis gyroscope. In order to demonstrate the proposed control strategy, this paper adopts two proportional-integral controllers: one for regulating flow-relative speed and the other for turning rate. We have

$$A_b = K_P^A (U_d - \tilde{U}) + K_I^A \int U_d - \tilde{U} dt, \quad (34)$$

$$B_b = K_P^B (\omega_d^U - \tilde{\omega}^U) + K_I^B \int \omega_d^U - \tilde{\omega}^U dt, \quad (35)$$

where A_b and B_b are the feedback components of control variable A and B , respectively, $\tilde{\omega}^U = \tilde{\omega} - \dot{\tilde{\alpha}}$ is the estimated flow-relative turning rate, and K_P^A , K_I^A , K_P^B and K_I^B are the controller parameters. $\dot{\tilde{\alpha}}$ is computed by differentiation of the angle-of-attack Bayesian estimate.

VI. SIMULATION RESULTS

Simulations were conducted to test the proposed flow-relative-control scheme. The fish robot tunes the sinusoidal oscillation amplitude A and bias rate B in the internal-reaction-wheel spinning profile to track reference signals of swimming speed U_d and turning rate ω_d^U based on flow estimates and angular velocity measurements. We simulate flow-relative path following in a uniform flow. The control calculation occurs at the beginning of each oscillation period. The oscillation/flapping frequency is 0.75 Hz. The parameters of the fish robot is selected based on our previously-reported, lab-developed, servo-actuated prototype [7] (Table I).

Parameter	Value	Parameter	Value
m_1	1.0 kg	m_2	1.5 kg
C_{D0}	20 kg·m ⁻¹	C_D	500 kg·m ⁻¹
C_L	100 kg·m ⁻¹	K_H	0.2
k_1	0.356 g·m·s ⁻²	k_2	2
k_3	5.33 g·m·s ⁻²	k_4	2
J	0.01 kg·m ²	J_r	0.002 kg·m ²
C_p	1 kg	K_p	1 kg·m ² ·s ⁻¹

TABLE I: Model parameters used in simulation [7].

Figure 4 shows the robot trajectory in tracking a constant swimming speed and a stepped turning rate in a uniform flow

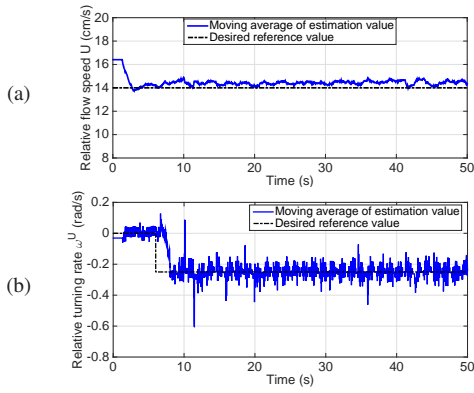


Fig. 5: The moving average of flow-relative speed U and turning rate ω^U with a time window size equal to one control period. (a) Flow-relative speed U ; and (b) flow-relative turning rate ω^U .

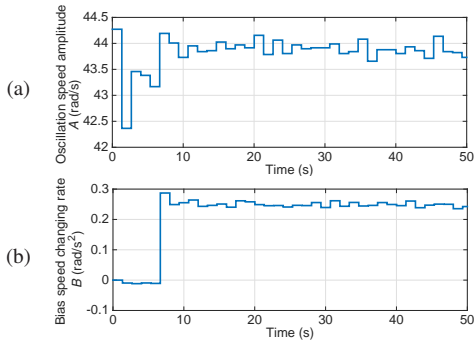


Fig. 6: The commanded control variables in the reaction-wheel angular velocity. (a) Sinusoidal oscillation amplitude A ; and (b) bias speed changing rate B .

of 1 cm/s in the x^1 direction. The red dots on the boundary of the fish robot represents the pressure sensors. The vortices in red rotate in the clockwise direction and the blue ones rotate in the counter-clockwise direction. The green dash-dot line indicates the swimming trajectory of the fish robot. Before 6 s, the desired flow-relative turning rate ω^U is zero, which means that fish robot travels straight in the same direction of the initial velocity, i.e., along the $-x^1$ -axis. After 6 s, the reference turning rate changes to -0.25 rad/s, which results in a circular trajectory relative to the flow. The controlled swimming speed converges to the desired reference value with less than 5% tracking error within two flapping periods (Fig. 5a). Although the turning-rate estimation is noisy, which comes from the derivative operation on the estimated angle-of-attack, the mean turning-rate estimate tracks the reference (Fig. 5b). The discrepancy in the estimated and ground-truth values may come from the quasi-steady potential flow model used in the estimation algorithm, which ignores the unsteady effects in the swimming motion. The control variables, the amplitude and the changing rate of reaction-wheel angular velocity are presented in Fig. 6.

VII. CONCLUSION AND FUTURE WORK

This paper presents the flow-relative control design of a flexible fish robot actuated by an internal reaction wheel. We study the dynamics of the fish robot and approximate the effects of the reaction wheel as an external torque acting on the fish robot. The reaction-wheel angular-velocity profile is designed to be a biased oscillating function for generating fish-like swimming motion. A Bayesian filter assimilates distributed pressure measurements and bending curvature measurement for state estimation. A control scheme combining feedforward and feedback is proposed for flow-relative path-following, i.e., tracking flow-relative swimming-speed and turning-rate references. Simulation results of flow-relative path following in a uniform flow are presented to further demonstrate the proposed strategy.

In ongoing work, we are testing this flow-relative control strategy with a flexible fish robot using a two-dimensional testbed that is under development. In addition, it is of interest to apply the controller design to achieve vortex tracking and Karman-gaiting behaviors of a flexible fish robot.

REFERENCES

- [1] X. Tan, "Autonomous robotic fish as mobile sensor platforms: Challenges and potential solutions," *Marine Technology Society Journal*, vol. 45, no. 4, pp. 31–40, 2011.
- [2] V. Kopman and M. Porfiri, "Design, modeling, and characterization of a miniature robotic fish for research and education in biomimetics and bioinspiration," *Mechatronics, IEEE/ASME Transactions on*, vol. 18, no. 2, pp. 471–483, 2013.
- [3] P. Tallapragada, "A swimming robot with an internal rotor as a nonholonomic system," in *American Control Conference (ACC), 2015. IEEE*, 2015, pp. 657–662.
- [4] B. Bialke, "High fidelity mathematical modeling of reaction wheel performance," *Guidance and control 1998*, pp. 483–496, 1998.
- [5] S. Coombs, "Smart skins: information processing by lateral line flow sensors," *Autonomous Robots*, vol. 11, no. 3, pp. 255–261, 2001.
- [6] T. Salumäe and M. Kruusmaa, "Flow-relative control of an underwater robot," in *Proceedings of the Royal Society of London A: Mathematical, Physical and Engineering Sciences*, vol. 469, no. 2153. The Royal Society, 2013, p. 20120671.
- [7] F. Zhang, F. D. Lagor, D. Yeo, P. Washington, and D. A. Paley, "Distributed flow sensing for closed-loop control speed control of a flexible fish robot," *Bioinspiration & Biomimetics, Special Issue on Bio-inspired Soft Robotics*, vol. 10, no. 6, p. 065001, 2015.
- [8] L. DeVries, F. D. Lagor, H. Lei, X. Tan, and D. A. Paley, "Distributed flow estimation and closed-loop control of an underwater vehicle with a multi-modal artificial lateral line," *Bioinspiration & Biomimetics*, accepted for publication.
- [9] R. L. Panton, *Incompressible flow*. John Wiley & Sons, 2006.
- [10] X. Xia and K. Mohseni, "Lift evaluation of a two-dimensional pitching flat plate," *Physics of Fluids (1994-present)*, vol. 25, no. 9, p. 091901, 2013.
- [11] P. Holmes, J. Jenkins, and N. E. Leonard, "Dynamics of the Kirchhoff equations I: Coincident centers of gravity and buoyancy," *Physica D: Nonlinear Phenomena*, vol. 118, no. 3, pp. 311–342, 1998.
- [12] J. D. Anderson, *Aircraft performance and design*. McGraw-Hill New York, 1999, vol. 1.
- [13] F. D. Lagor, L. D. DeVries, K. M. Waychoff, and D. A. Paley, "Bio-inspired flow sensing and control: Autonomous rheotaxis using distributed pressure measurements," *Journal of Unmanned System Technology*, vol. 1, no. 3, pp. 78–88, 2013.
- [14] S. Särkkä, *Bayesian filtering and smoothing*. Cambridge University Press, 2013, vol. 3.
- [15] X. Tan, M. Carpenter, J. Thon, and F. Alequin-Ramos, "Analytical modeling and experimental studies of robotic fish turning," in *Robotics and Automation (ICRA), 2010 IEEE International Conference on. IEEE*, 2010, pp. 102–108.